Research on Engineering Structures & Materials
www.jresm.org
MIM Research Group

Research Article

Flexural behavior of bamboo reinforced geopolymer concrete slabs using sodium silicate waste and copper slag for sustainable construction

Balamurali Kanagaraj [*,1,a], Arkishembha Sohliya [1,b], Jayakumar G [2,c], Varun Sabu Sam [1,d], N. Anand [1,e], Marc Azab [3,f]

[1]*Department of Civil Engineering, Karunya Institute of Technology and Sciences, Coimbatore, India*
[2]*Department of Civil Engineering, Sri Krishna College of Technology, Coimbatore, India*
[3]*College of Engineering and Technology, American University of the Middle East, Egaila, 54200, Kuwait*

Article Info

Article History:

Received 21 June 2026
Accepted 12 July 2026

Keywords:

Bamboo reinforcement; Geopolymer concrete; Copper slag; Structural performance; Sustainable construction

Abstract

The aim of this experimental study is to evaluate the flexural behavior of bamboo-reinforced geopolymer concrete (GPC) slabs incorporating industrial by-products as sustainable alternatives to conventional reinforced concrete. To reduce the environmental impact associated with Portland cement, steel reinforcement, and natural aggregates, geopolymer concrete reinforced with treated bamboo was developed using sodium silicate waste (SSW) as a 40% replacement for coarse aggregate and copper slag (CS) as a 50% replacement for fine aggregate. Four slab panels, namely bamboo-reinforced cement concrete, bamboo-reinforced geopolymer concrete (GPC), SSW-blended GPC, and CS-blended GPC, were fabricated and tested under simulated uniformly distributed loading. The structural response was evaluated in terms of load-deflection behavior, first-crack load, ultimate load, stiffness, ductility index, deformability factor, and energy absorption capacity. Compared with the cement control, the GPC slab increased the first-crack load by 26% and the ultimate load by 8%. The SSW-blended GPC slab achieved an ultimate load of 50 kN and exhibited the highest ductility index (4.20), while the CS-blended GPC slab demonstrated the best overall structural performance with the highest ultimate load (52 kN, 6% higher than the GPC slab), stiffness (12.3 kN/mm), and energy absorption capacity (1748 kNmm). The results demonstrate that integrating alkali-activated binders, industrial by-products, and bamboo reinforcement can produce structurally efficient and environmentally sustainable slab systems. Among the investigated mixes, the CS-blended geopolymer slab exhibited the most balanced combination of strength, stiffness, and toughness, highlighting its potential for sustainable structural applications.

1. Introduction

Rapid infrastructure growth continues to drive global demand for construction materials, and this rising demand is accelerating the overexploitation of finite natural resources [1], with consequent environmental degradation of the surrounding ecosystems. To curb the consumption of virgin materials in concrete production, researchers are increasingly substituting a range of industrial by-products for natural constituents [2]. Construction and demolition (C&D) waste, one of the most abundant waste streams generated by the construction sector, is a widely studied substitute for

*Corresponding author: balakmurali31@gmail.com
[a]orcid.org/0000-0003-3006-370X; [b]orcid.org/0000-0002-4189-3568; [c]orcid.org/0000-0001-5348-6452; [d]orcid.org/0009-0004-7954-0292; [e]orcid.org/0000-0001-7643-9747; [f]orcid.org/0000-0003-0173-3209
DOI: http://dx.doi.org/10.17515/resm2026-1771ma0621rs

conventional aggregates [3]. Because this stream contains a heterogeneous mixture of concrete debris, scrap steel, plastics, and broken brick bats, suitable refining and separation techniques are required to remove the unwanted matter before reuse [4]. The behavior of concrete incorporating recycled concrete aggregate (RCA) therefore warrants careful study, particularly under harsh exposure conditions, as RCA exhibits higher porosity and water absorption along with lower abrasion resistance than virgin aggregates [5]. From an economic standpoint, higher RCA contents lower production costs, with a fully recycled (100% RCA) mix reported to be roughly 31% cheaper to produce [6]. However, using RCA as fine aggregate reduces strength at high replacement levels, with a replacement of about 30% reported as the optimal balance [7]. Copper slag (CS) mixes likewise show higher drying-shrinkage strain than virgin-aggregate concrete, although the values remain within acceptable limits [8]. The use of recycled materials and industrial by-products as an alternative to conventional coarse aggregate is increasing to enhance the sustainability of the concrete [9–13].

The origin of the parent concrete strongly influences the strength of RCA mixes when the replacement ratio is high [14]. Full replacement of virgin aggregate with RCA has been reported to reduce flexural strength by about 3% and 11% for M30 and M50 grade mixes, respectively [15]. Conversely, RCA has been found to enhance shear strength, supporting its suitability for sustainable structural applications [16]. The bond strength between RCA concrete and steel reinforcement is largely independent of RCA content, and complete replacement of virgin aggregate can still yield satisfactory mechanical performance [17]. At higher replacement levels, the strength penalty becomes significant—reported as 21% to 44% strength loss for a 70% RCA mix—although the addition of fibres can offset this by improving durability [18]. Similarly, incorporating nanomaterials such as nano-silica at dosages up to 3% can raise the compressive and flexural strength of a 100% RCA mix by as much as 22% and 26%, respectively [19].

Beyond aggregate consumption, the production of Portland cement is highly resource-intensive and a major source of anthropogenic carbon emissions [20]. The manufacture of one ton of cement releases approximately one ton of greenhouse gases [21]. Rising greenhouse-gas concentrations contribute to environmental degradation, including global climate change and rising temperature gradients worldwide [22]. These concerns make the transition to low-impact binders imperative. Geopolymer concrete (GPC), which eliminates the need for cement, is one of the most promising alternatives [23]. GPC is produced by activating alumina- and silica-rich precursors with an alkaline solution [24]. Unlike cement concrete, GPC can develop strength under ambient curing, while elevated-temperature curing further accelerates strength gain [25].

The strength of GPC is governed by several interacting factors, including the alkaline activator ratio, sodium hydroxide molarity, curing temperature and duration, the type of precursor, and the overall mix proportions [26,27]. Strength can be enhanced by adding high-calcium materials such as slag or metakaolin and by elevated-temperature curing [28,29]. At the structural scale, the load-carrying behavior of GPC has generally been found comparable to that of their cement-concrete counterparts [30–32]. From a life-cycle perspective, the global warming potential of GPC has been reported to be about 64% lower than that of cement concrete [33]. Its bond strength has also been shown to remain comparable to conventional concrete after exposure to 300 °C [34]. Interest in GPC is increasing because of the use of industrial by-products from various sources [35–38].

A parallel strategy for improving sustainability is the use of natural reinforcing materials in place of steel [39]. Among these, bamboo is a particularly attractive substitute for steel in low-cost housing owing to its rapid renewability, wide availability, and favorable strength-to-weight ratio [40]. Reported bamboo properties include a yield strength of about 101 MPa—roughly 25% that of Grade 60 steel—and an elastic modulus of about 19 GPa, approximately 10% that of steel [41]. Ramaani et al. [42] examined the structural integrity of bamboo-reinforced elements and reported that bamboo-reinforced slabs behave similarly to steel-reinforced specimens. Untreated bamboo-reinforced and plain concrete elements both fail in a brittle manner, whereas elements made with treated bamboo behave in a ductile fashion; at a reinforcement ratio of about 8%, bamboo-reinforced members performed comparably to steel-reinforced members under axial and transverse loading [43]. Proper seasoning and surface treatment are essential to develop adequate bond strength between bamboo and the surrounding matrix [44]. The choice of binder also matters: bamboo-reinforced cement concrete has been reported to outperform an equivalent steel-reinforced mix by about 6.5%, whereas fly ash (FA)- and slag-based mixes performed below the reference [45]. Overall, bamboo-reinforced beams perform close to steel-reinforced beams, with only marginal reductions of about 2.8% and 3.2% in the first crack load and ultimate load relative to steel-reinforced elements [46]. Table 1 shows the experimental findings of bamboo-reinforced concrete elements. For columns, the ductility of bamboo-reinforced members depends largely on the compressive strength of the mix [47]. Bamboo also offers good ductility and shear resistance; in shear-wall applications, bamboo-reinforced sections have performed comparably to steel-reinforced sections [48].

Table 1. Literature collection on the bamboo-reinforced concrete elements

Reference	Materials/Methods	Findings
[49]	Flexural behavior of concrete slabs	Bamboo reinforcement has been shown to increase the load-carrying capacity of slab elements relative to unreinforced reference specimens.
[50]	Flexural behavior of concrete beams reinforced with bamboo strips	The bamboo reinforcement ratio strongly affects beam performance: a ratio of about 2.8% gave the best shear and flexural response, outperforming beams reinforced at 3.8%.
[51]	Flexural behavior of concrete beam	The ultimate load of the bamboo-reinforced concrete (BRC) beam was equivalent to that of the reinforced cement concrete (RCC) beam after 14 and 28 days; in addition, the BRC beam deflected more than the RCC beam.
[52]	Flexural behavior of concrete slabs	Bamboo-reinforced slabs can achieve 82% of the strength and 93% of the ductility compared to steel-reinforced concrete (SRC) slabs, suggesting bamboo is a promising substitute for steel.
[53]	Flexural behavior of concrete beam	The average flexural strength for BRC beams was significantly lower (82.8% reduction) than SRC beams, whereas the hybrid configuration with bamboo in compression and steel in tension showed the most promising results.
[54]	Flexural behavior of concrete beam	Use of acetic acid treatment to enhance bamboo's properties, resulting in a 32.56% reduction in water absorption and a 17% increase in tensile strength compared to untreated bamboo.
[55]	Concrete reinforced with bamboo fiber	Optimal bamboo fiber dosage of 0.25% increased splitting tensile strength by 21.74% and flexural strength by 12.13%, which could reduce ground floor slab thickness by nearly 20%.
[56]	Flexural behavior of concrete slabs	The flexural strength of BRC specimens decreased by 15%, but with a weight advantage of 20% less compared to normal reinforced concrete slabs of the same dimension.
[57]	Flexural behavior of concrete beam	Treating the bamboo with epoxy and binding wire significantly improves the flexural and bond strength compared to untreated bamboo or bamboo treated only with epoxy or bitumen emulsion.
[58]	Flexural behavior of concrete beam	Beams with bamboo reinforcement coated with water-resistant material and hose clamps show increased flexural capacity, ductility, and stiffness compared to other treated and untreated specimens.

Although considerable research has been conducted on geopolymer concrete, bamboo reinforcement, and the utilization of industrial by-products, these studies have primarily examined each sustainable component independently. The combined structural behavior of bamboo-reinforced geopolymer concrete slabs incorporating both sodium silicate waste as coarse aggregate and copper slag as fine aggregate remains largely unexplored. Furthermore, previous studies have predominantly focused on material characterization or individual structural components, with limited attention given to the overall flexural response, stiffness, ductility, deformability, and energy absorption of sustainable slab systems. Consequently, the synergistic interaction between these sustainable materials and their influence on structural performance has not yet been comprehensively established.

The primary objective of this study is to evaluate the flexural behavior of bamboo-reinforced geopolymer concrete slabs incorporating sodium silicate waste and copper slag as partial replacements for natural aggregates. The novelty of this research lies in the integrated development and structural assessment of a sustainable slab system that simultaneously replaces Portland cement, steel reinforcement, and natural aggregates with low-carbon alternatives. Four slab configurations, namely bamboo-reinforced cement concrete (cement mix), bamboo-reinforced geopolymer concrete (GPC mix), bamboo-reinforced sodium silicate waste-blended geopolymer concrete (SSW mix), and bamboo-reinforced copper slag-blended geopolymer concrete (CS mix), were experimentally investigated under uniformly distributed loading. The load-deflection response, first-crack load, ultimate load, stiffness, ductility index, deformability factor, and energy absorption capacity were systematically evaluated to establish the structural feasibility and engineering potential of this integrated sustainable construction approach.

2. Materials

2.1. Binder

For the GPC mix, Low-calcium fly ash (FA) and ground granulated blast-furnace slag were used as the binders, with the FA-to-slag ratio fixed at 70:30 to promote early setting and strength gain at room temperature. The oxide composition of the binder materials is shown in Table 2. The FA was sourced from a thermal power plant and the slag from JSW Steel. For cement concrete, Portland pozzolana cement was used as the primary binder material for the development of concrete.

2.2 Aggregate

Manufactured sand (M-sand) and crushed coarse aggregate were used, with maximum particle sizes of 4.75 mm and 10 mm and specific gravities of 2.6 and 2.72, respectively; the oxide composition of SSW was given in Table 2. This waste was collected, processed in the laboratory, and identified as a viable coarse-aggregate substitute.

Table 2. The oxide composition of FA, GGBFS, and SSW [60]

Oxides	FA (%)	Slag (%)	SSW (%)
SiO_2	61.2	42.4	53.47
Al_2O_3	26.9	13.2	–
$CaCO_3$	-	-	26.43
$NaAlSi_3O_8$	–	–	3.14
Br	–	–	0.31
Sr	–	–	2.09
Fe_2O_3	6.21	1.12	0.31
CaO	1.91	41.2	–
MgO	0.29	1.3	–
Na_2O	0.58	0.3	–
K_2O	1.21	0.7	–
Ti	0.4	–	–

Because it derives from sodium silicate, the SSW contains free silica that can enhance geopolymerization and the performance of GPC. Following previous work [59], the SSW replacement was fixed at 40% of the coarse aggregate. Like conventional coarse aggregate, the SSW had a particle size of 10–12.5 mm and a specific gravity of 2.65. The fine aggregate was partially replaced with copper slag (CS) at 50% by mass; the CS had a specific gravity of 2.62. A water-to-cement (w/c) ratio of 0.4 was used for the cement mix, and a water-to-binder (w/b) ratio of 0.6 for the GPC mixes, as shown in Table 3. Figure 1 shows the particle size distribution of the aggregates used in the study. For the SSW mix, the mixing water was increased by 5% to compensate for the additional absorption by the industrial by-products.

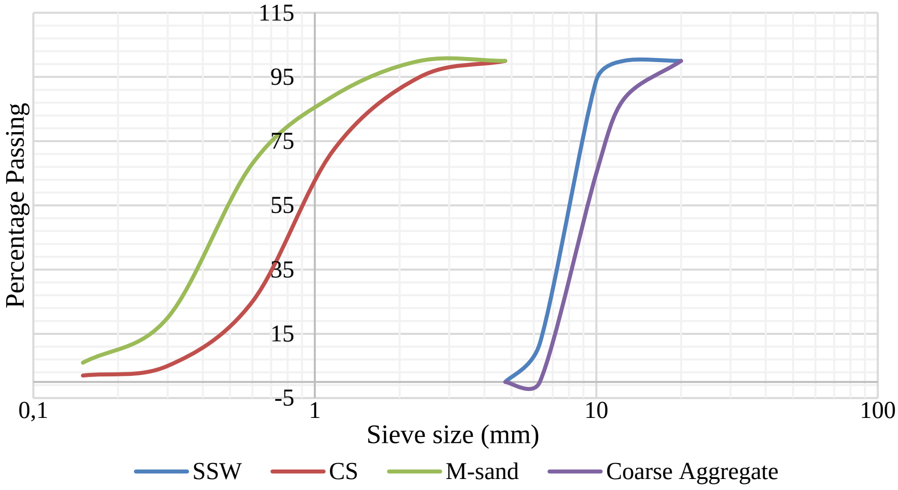

Fig. 1. Particle size distribution of aggregates

2.3 Activator

Industrial-grade sodium hydroxide and sodium silicate were combined in a 1:2 ratio, with the sodium hydroxide prepared at a concentration of 12 M. The activator solution was mixed one hour before casting to allow the reaction to begin.

2.4 Bamboo

The reinforcement used was Dendrocalamus hamiltonii bamboo, selected for its abundance in southern India—an estimated 0.45 million hectares of Tamil Nadu are under bamboo cover. After treatment, the bamboo developed a tensile strength of 200 MPa. The bamboo strips used to reinforce the slabs were 7 mm thick and 10 mm wide.

Table 3. Mix design

Sl. No	Cement	FA	GGBS	M-sand	Coarse aggregate	SSW	CS	Sodium Hydroxide	Sodium Silicate
					(kg/m³)				
1.	-	250	250	890	1080	-	-	89	134
2.	-	250	250	890	648	432	-	89	134
3.	-	250	250	445	1080	-	445	89	134
4.	410	-	-	890	1050	-	-	-	-

3. Experimental Methods

Following the mix proportions in Table 3, the concrete was batched in the laboratory and cast into moulds measuring 1 m (length) × 0.7 m (width) × 0.075 m (depth), as shown in Figure 2. The cement specimens were moist-cured under wet gunny bags, while the GPC specimens were cured under ambient conditions. The slabs were tested in a 50-tonne loading frame; to distribute the applied load across the top surface, a dedicated load-transfer platform was used (Figure 3). The loading arrangement and test setup are shown schematically in Figure 4.

(a) (b)

Fig. 2. (a) Bamboo strips; (b) Bamboo reinforced slab panels

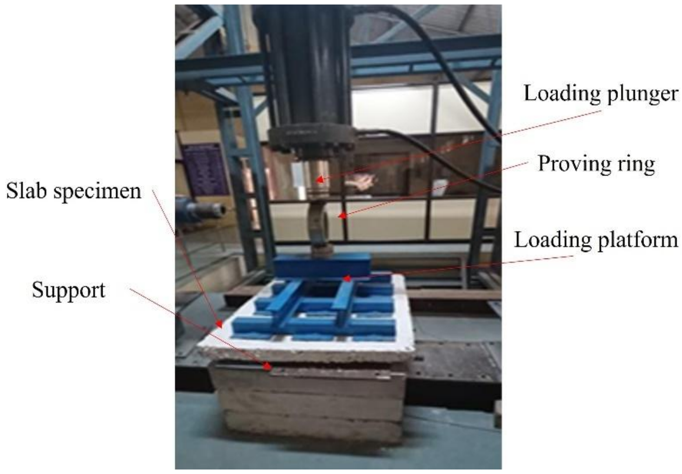

Fig. 3. Testing of slab specimens

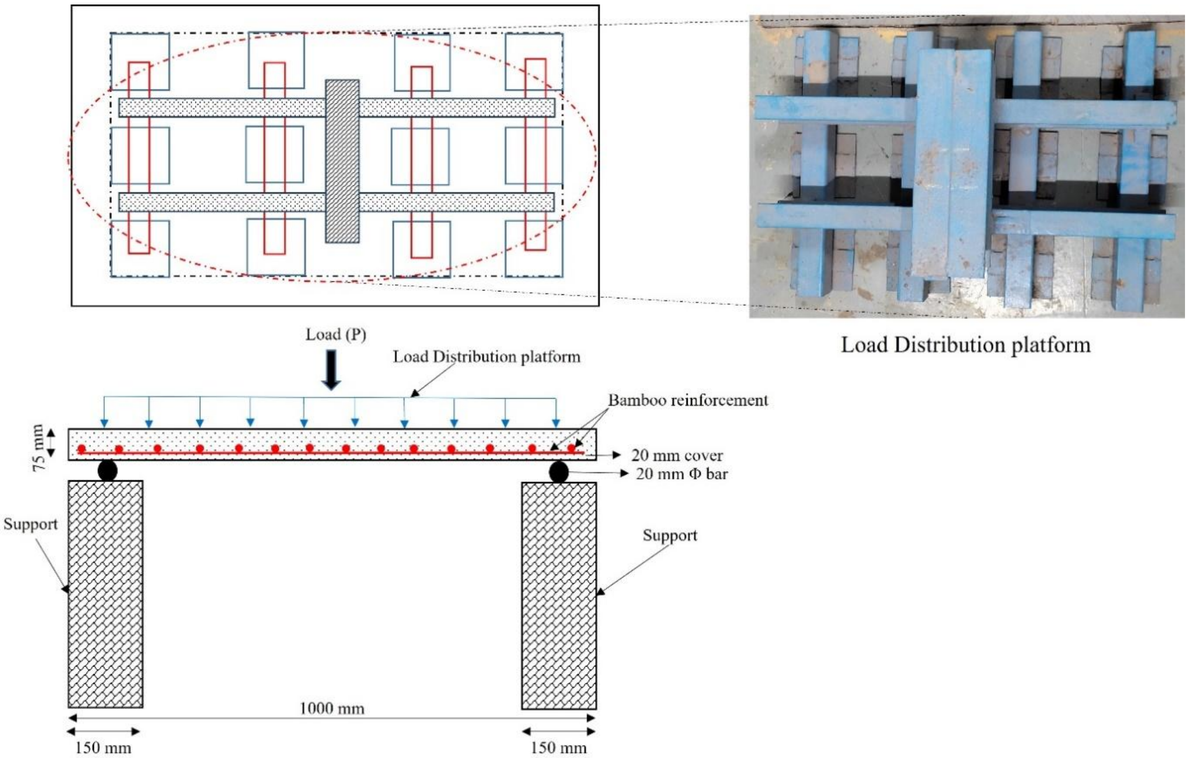

Fig. 4. Schematic representation of the test setup

4. Results

4.1. Workability

The fresh behavior of each mix was assessed by the slump-cone test, in which the cone was filled in layers and compacted to expel entrapped air; the drop in height after lifting the cone was recorded as the slump value, following ASTM C143 [61]. The cement mix recorded the highest slump, at 80–85 mm. The GPC mix was slightly lower at 70–75 mm, while the SSW-blended mix gave the lowest slump (68–70 mm), reflecting the additional water absorbed by the porous waste particles. The CS-blended mix returned to 70–75 mm, comparable to the plain GPC mix. The average slump value is represented in Figure 5.

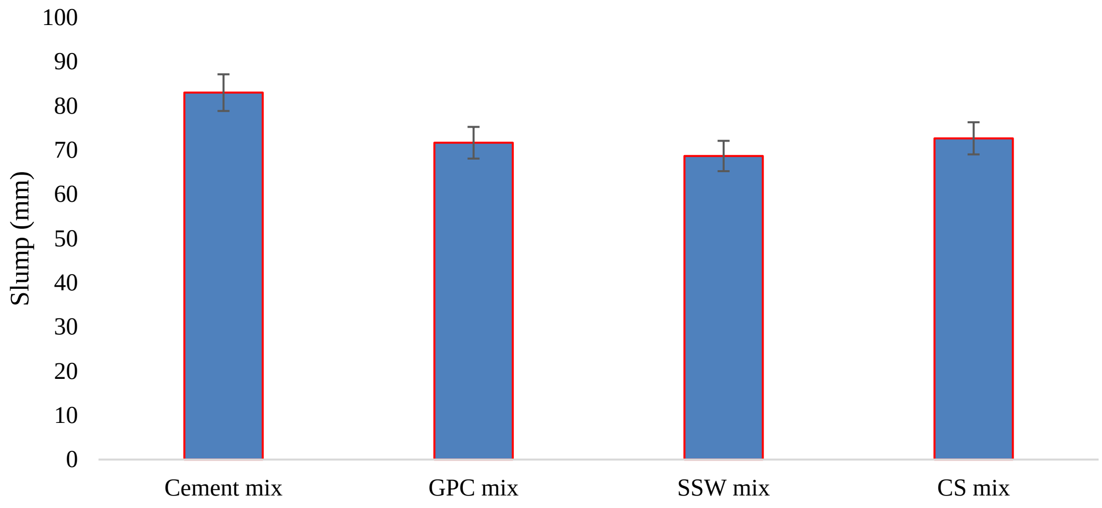

Fig. 5. Slump value of the concrete mixes

4.2. Compressive Strength

The hardened specimens were tested to confirm that they reached their target strength, following IS 516 [62]. The cement concrete attained a 28-day compressive strength of 34 MPa, while the GPC reached 36 MPa under ambient curing, confirming that alkali activation and geopolymerization proceeded efficiently and slightly exceeded the cement control. The SSW-blended GPC developed 32 MPa, an 11% reduction relative to the plain GPC, attributable to the heterogeneous, porous nature of the waste particles.

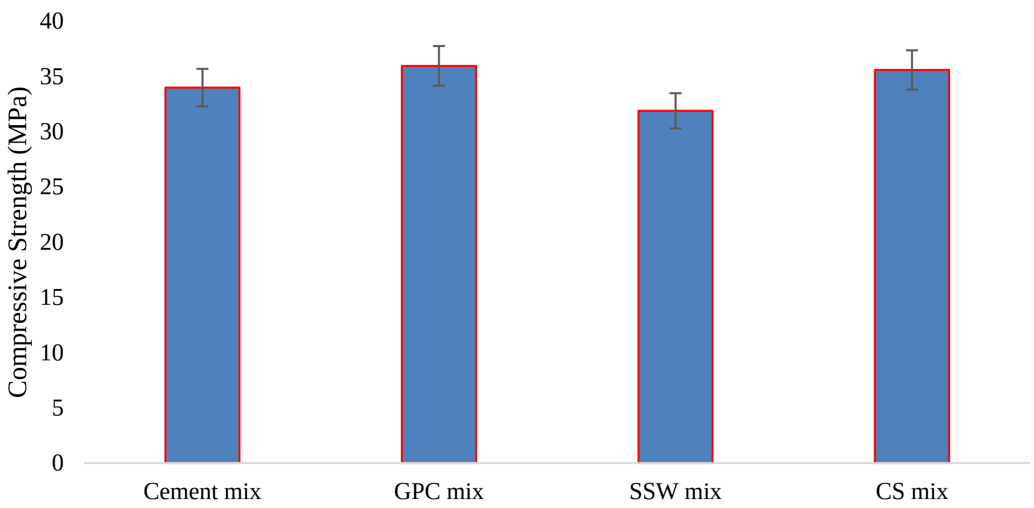

Fig. 6. Compressive strength of the concrete mixes

The average compressive strength of all the mixes was plotted in Figure 6. Table 4 shows the statistical analysis of the compressive strength of the concrete mixes. The CS-blended GPC achieved 35.6 MPa, comparable to the plain GPC, which is consistent with the dense particle packing provided by the angular slag. Overall, substituting natural constituents with industrial by-products preserved the target strength while improving the sustainability of the mixes.

Table 4. Statistical analysis of the compressive strength of the concrete mixes

Specimen type	Trial 1	Trial 2	Trial 3	Mean	σ	CoV (%)
Cement mix	33.6	34.5	33.8	34	0.47	0.0139
GPC mix	37.3	35.4	35.1	36	1.19	0.0332
SSW mix	33.4	30.8	31.4	32	1.36	0.0427
CS mix	36.8	34.4	35.5	35.6	1.20	0.0338

**Note: σ - Standard Deviation, CoV - Coefficient of Variation (%)*

4.3 Load-Deflection Behavior

Each slab was simply supported on all four edges and loaded through the load-transfer platform so that the applied force was distributed across the top surface. The load was applied from the loading frame and monitored with a proving ring, which also allowed the loading rate to be controlled, while mid-span deflection was recorded with a dial gauge positioned at the bottom center of the slab. Figure 7 presents the load–deflection response of the four mixes. The cement mix exhibited the flattest profile, indicating the lowest resistance to load because of its brittleness and lower matrix density. The GPC and CS mixes showed similar load–deflection profiles, indicating comparable structural behavior; the dense, angular CS particles raise packing density and internal friction, which improves the response under load.

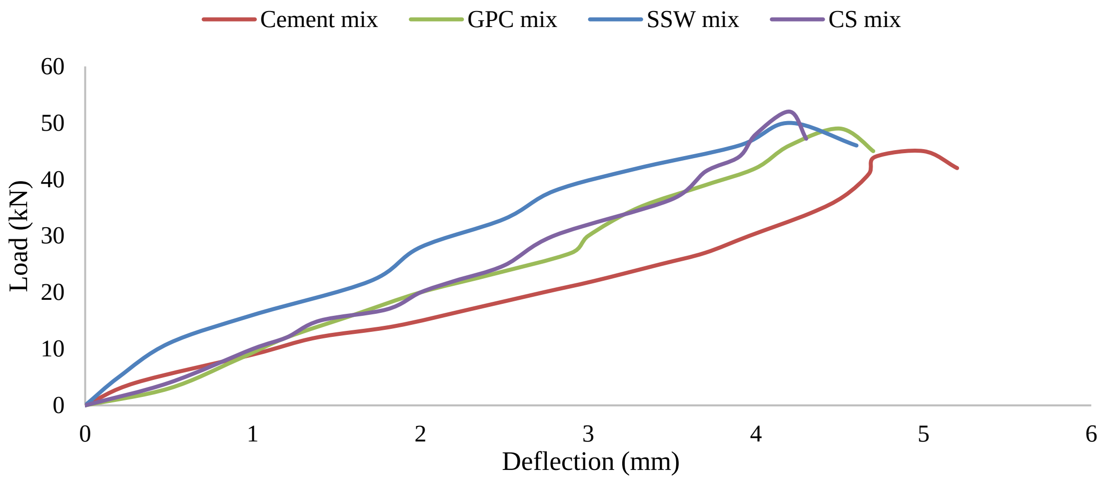

Fig. 7. Load-Deflection behavior

The SSW-blended mix produced the steepest load–deflection profile of all specimens, signifying the greatest resistance to load, which is consistent with the chemically reactive nature of the waste. The maximum recorded deflections were 5.2 mm for the cement mix (the lowest stiffness and load capacity), 4.5 mm for the GPC mix, and 4.2 mm for both the CS- and SSW-blended mixes, reflecting their superior resistance to deflection. The reactive silica supplied by the SSW promotes additional gel formation [60], producing a denser matrix and an improved interfacial transition zone (ITZ) that limits micro-cracking and raises the load-carrying capacity, while the reduced deflection points to increased stiffness through the formation of a more rigid microstructure.

4.4 First crack load

The first-crack load was examined to assess the cracking resistance of the slabs. Figure 8 presents the first-crack loads of the four mixes. The cement mix cracked at 17 kN, providing the baseline for comparison. The GPC mix performed best, with a first-crack load of 23 kN—26% higher than the cement mix—owing to its dense, cohesive alumina-silicate gel matrix and stronger ITZ, which restrict micro-cracking and allow the slab to sustain higher stress before cracking. By contrast, the SSW mix cracked at only 16 kN, 30% below the GPC mix, because the heterogeneous particle size and reactive nature of the SSW favor ultimate load capacity rather than early flexural cracking resistance. The CS mix cracked at 17 kN, equal to the cement mix and 26% below the GPC mix; the angular CS particles enhance mechanical interlock and overall strength but contribute little tensile-cracking resistance at early stages. Being largely inert, the CS improves compressive strength more than tensile or flexural strength, which limits its first-crack performance. These results highlight the marked variation in cracking resistance among the mixes.

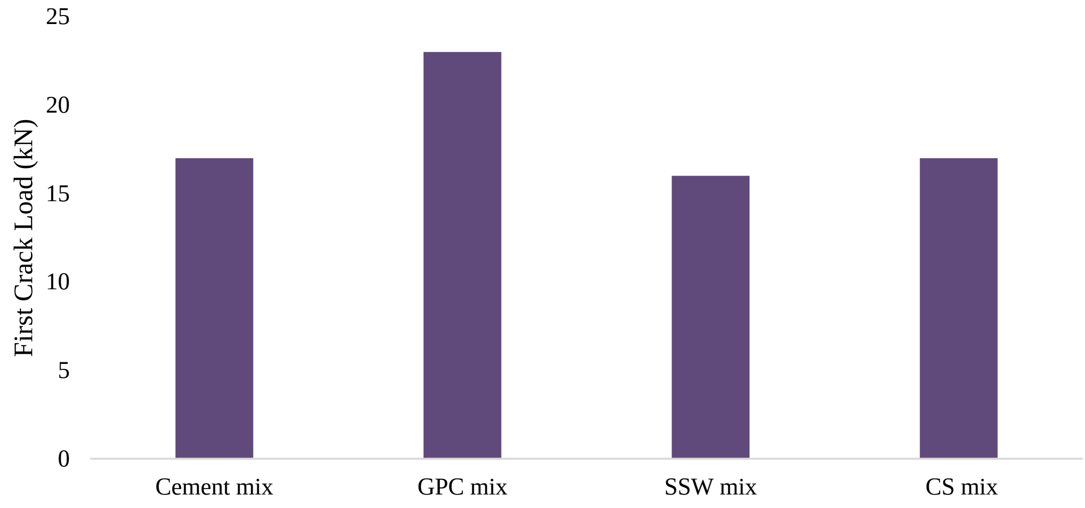

Fig. 8. First Crack load of the Slab elements

4.5 Ultimate Load

The ultimate loads of the slabs are shown in Figure 9. The cement mix carried the lowest ultimate load, 45 kN, because cement concrete offers limited resistance to crack propagation under flexure and tends to fail prematurely; the ITZ is the critical region where micro-cracking initiates under high stress. The GPC mix reached 49 kN, 8% above the cement control, reflecting its stronger ITZ and improved aggregate–matrix adhesion from the alumina-silicate gel phases, which delay crack progression and allow the slab to sustain higher loads before failure.

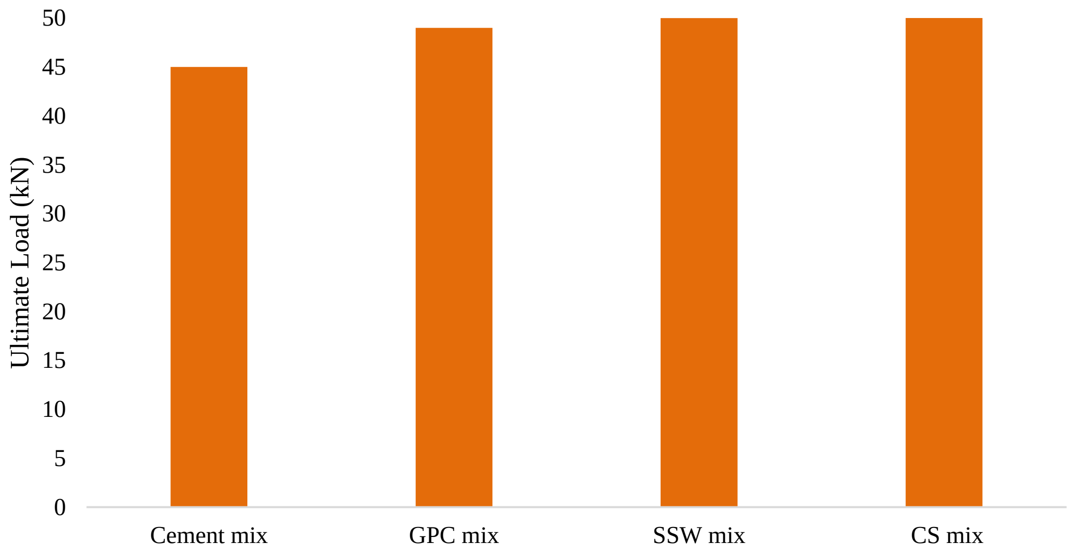

Fig. 9. Ultimate load of the Slab elements

The SSW mix carried 50 kN, marginally (2%) above the GPC mix, because the SSW acts as a supplementary silicate source that promotes secondary gel formation and pore filling [60], producing a denser matrix that improves stress transfer and redistribution and delays failure after first cracking. The CS mix gave the highest ultimate load, 52 kN—6% above the GPC mix—as the dense packing of the angular CS particles improves particle interlock and compaction, reducing porosity and producing a stiffer matrix with enhanced compressive and flexural capacity; under high stress, the improved packing transfers load effectively and resists micro-crack widening by acting as a physical barrier. In summary, GPC offers a clear advantage over the cement mix, while the SSW and CS mixes provide superior load capacity, with the CS mix achieving the highest strength of all four specimens.

4.6 Stiffness

Stiffness was evaluated to characterize resistance to deformation under load, using Equation 1, and the results are shown in Figure 10. The cement mix had the lowest stiffness, 9 kN/mm, reflecting its high porosity, lower matrix density, and weak ITZ, which make it more prone to elastic and inelastic deformation and lead to larger deflections. The GPC mix reached 10.8 kN/mm, 17.3% higher than the cement mix, owing to its denser matrix; unlike the C-S-H of cement concrete, the alumina-silicate gel of GPC forms a more rigid molecular network that increases mechanical interlock and bond strength while lowering porosity, thereby offering moderate deformation resistance. The SSW mix attained 12 kN/mm, 8.5% above the GPC mix; despite its lower first-crack load, the reactive silicate source improves resistance to deformation and yields stiffer behavior under load. The CS mix recorded the highest stiffness, 12.3 kN/mm, 12% above the GPC mix, attributable to its superior particle packing, which improves mechanical interlock, reduces porosity, and strengthens the ITZ to produce a more rigid composite and minimize deflection. Stiffness therefore increased progressively from the cement mix to the CS mix, with the SSW and CS mixes providing the greatest rigidity.

$$k = \frac{P}{\Delta} \tag{1}$$

Where k is the stiffness, P is the ultimate load, and Δ is the deflection.

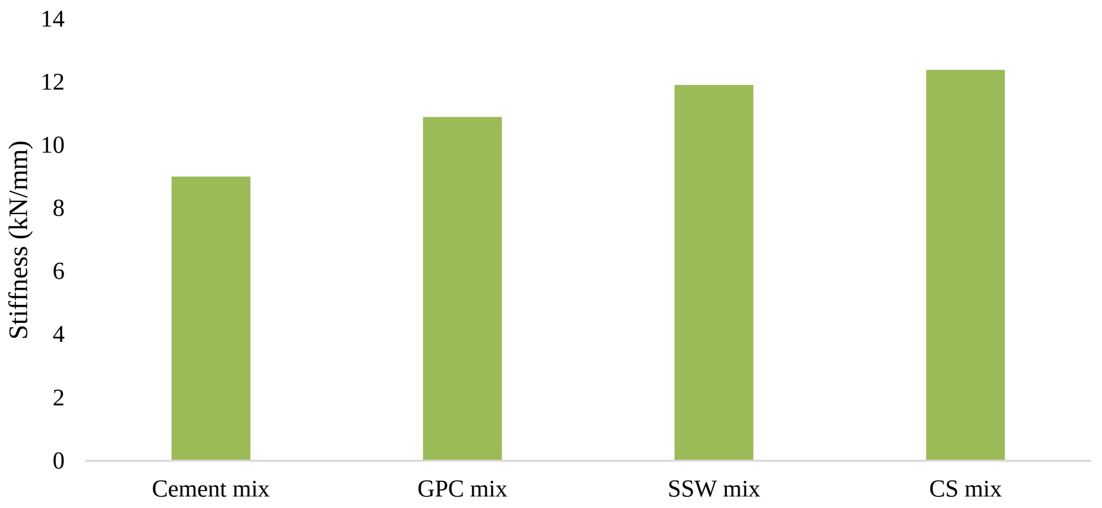

Fig. 10. Stiffness of the Slab elements

4.7 Ductility Index

The ductility index, which describes the deformation capacity before failure, was calculated using Equation 2, and the results for all four mixes are shown in Figure 11. The cement mix had a ductility index of 2.17, consistent with the gradual development and distribution of micro-cracks across the section as cement concrete passes through elastic and plastic stages before reaching ultimate load. The GPC mix had a lower index of 1.88, indicating more brittle behavior; the reduced ductility reflects its dense, rigid microstructure and suggests that GPC may fail with less warning and reduced visible cracking. The SSW mix recorded a markedly higher index of 4.20, 55% above the GPC mix, indicating superior flexibility and deformation capacity. This substantial increase suggests that the SSW alters the internal structure of the geopolymer matrix, promoting localized yielding and micro-crack propagation that improve energy dissipation during loading (Section 4.9). The CS mix had an index of 2.33, 20% above the GPC mix, a moderate improvement associated with the dense CS particles. Overall, the SSW mix exhibited by far the highest ductility, while the CS mix improved on the cement and GPC mixes but to a lesser degree.

$$DI = \frac{\Delta_u}{\Delta_f} \tag{2}$$

Where DI is the ductility index, Δ_u is the deflection at ultimate load and Δ_f is the deflection at the first crack.

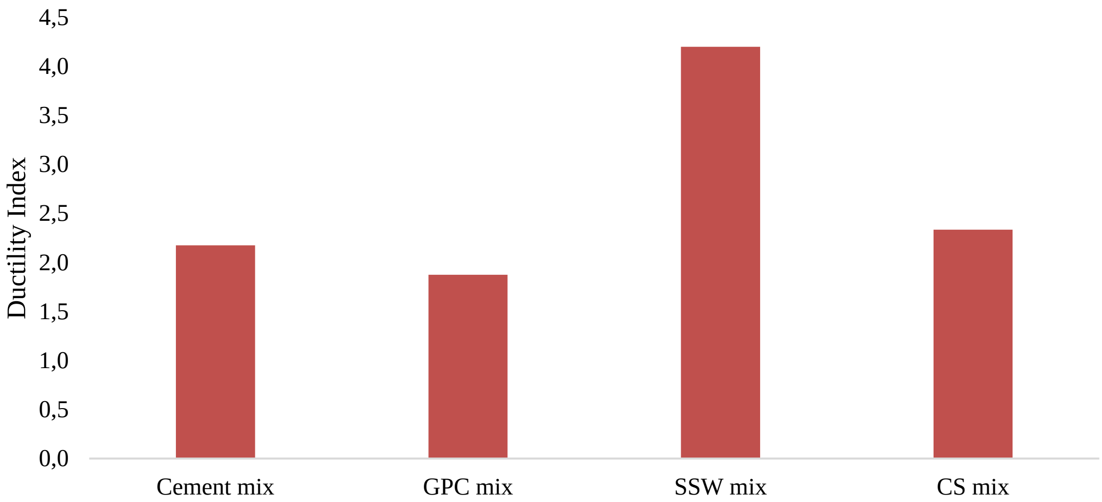

Fig. 11. Ductility Index of the Slab elements

4.8 Deformability factor

To complement the ductility index, the deformability factor was determined in accordance with CSA S806 [63], which characterizes a material's ability to sustain and redistribute stress after cracking. The results are shown in Figure 12.

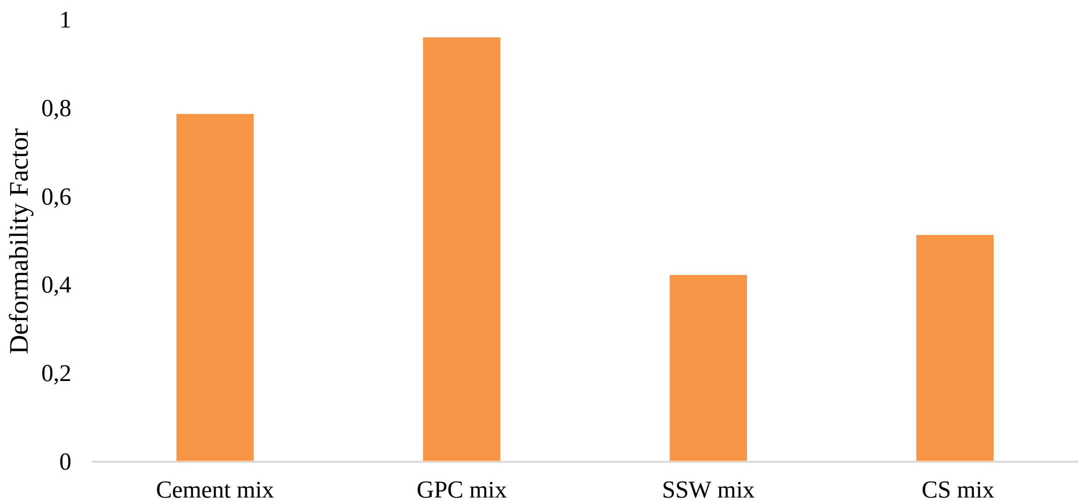

Fig. 12. Deformability factor of the Slab elements

The GPC mix recorded the highest deformability factor, 0.96, reflecting its strong alumina-silicate network, which retains structural integrity and accommodates considerable strain even after cracking. The cement mix had a factor of 0.78, 18% below the GPC mix; it offers adequate toughness but is limited by its brittleness and micro-cracking tendencies, which concentrate stress and precipitate failure, although its deformability still exceeds that of the CS and SSW mixes, indicating more balanced post-crack behavior.

Notably, although the SSW mix had the highest ductility index, it recorded the lowest deformability factor of all specimens, 0.42, which is 56% below the GPC mix. This apparent contradiction indicates that, while the SSW specimen can undergo large deflections, its post-yield strain distribution is limited, most likely because deformation localizes early. The CS mix gave a deformability factor of 0.51, 47% below the GPC mix; despite its strong performance in strength and stiffness, this low value points to a more brittle failure beyond peak load.

4.9 Energy Absorption capacity (EAC)

The energy absorption capacity (EAC), taken as the area under the load–deflection curve, was used to quantify each mix's ability to absorb and dissipate energy during loading (Figure 13). The cement mix recorded an EAC of 1718 kNmm, sustaining considerable load and deflection by dissipating energy through crack development, strain hardening, and aggregate interlock. The GPC mix, despite its higher strength and stiffness, gave a lower EAC of 1548 kNmm, 10% below the cement mix, indicating reduced energy-dissipation potential. The SSW mix recorded the lowest EAC, 1330 kNmm, 14% below the GPC mix and 22.6% below the cement mix; thus, despite its high ductility index, its capacity to absorb and store energy during loading was poor. The CS mix achieved the highest EAC, 1748 kNmm, 11.4% above the GPC mix and 1.7% above the cement mix, combining strength, stiffness, and sufficient post-crack deformation, which makes it effective at resisting sudden loads. The GPC mix therefore showed moderate energy absorption, while the SSW mix showed the least among the four specimens.

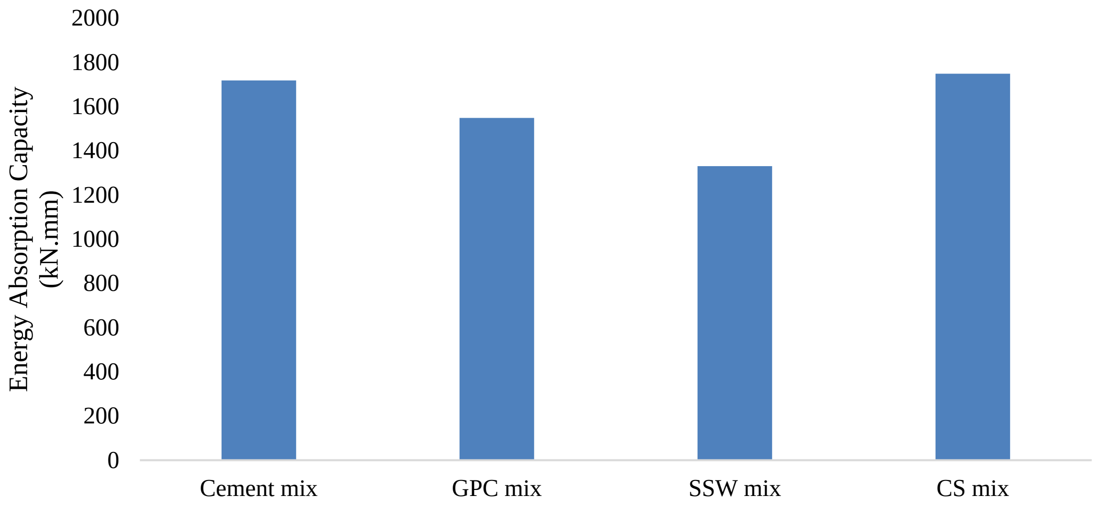

Fig. 13. EAC of the Slab elements

5. Discussion

The bamboo-reinforced cement slab provided the baseline against which the three geopolymer mixes were assessed, and the resulting failure patterns are shown in Figure 14. All four slabs failed in flexure, with cracks initiating at the bottom mid-span and propagating upward. The cement slab exhibited wider, more abrupt cracking, consistent with its brittle response and lower matrix density, whereas the geopolymer slabs developed finer, more distributed cracks before failure. Replacing cement with the FA–slag geopolymer binder improved almost every structural index, most notably the first-crack load, stiffness, and deformability factor, while only modestly lowering ductility and energy absorption. These results confirm that an alkali-activated binder can match or surpass conventional cement concrete in load-bearing performance while substantially reducing the embodied carbon of the slab [64,65]. Moreover, use of reactive coarse aggregates yields better performance in the concrete system [66], similar observations were seen when the conventional aggregate was replaced with Linz-Donawitz slag [67]. Whereas with the addition of basalt fiber to this Linz-Donawitz slag possess superior mechanical and durability property [68]. The use of fiber in the concrete mix with different proportions of industrial by-products tends to enhance the interfacial bonding, further resulting in attaining superior mechanical properties [69].

A recurring theme across the results is a trade-off between strength and energy-related ductility. Both by-product mixes raised the ultimate load and stiffness above the plain geopolymer slab, but they did so through distinct mechanisms with different consequences for post-peak behavior. In the SSW mix, the reactive free silica drives secondary gel formation and pore filling [60], yielding a chemically densified matrix; this is reflected in the steepest load–deflection profile and the highest ductility index (4.20). The angular copper slag, in contrast, acts primarily as a physical packing agent, densifying the matrix through improved particle interlock rather than through additional reaction product. This distinction explains why the CS slab combined the highest ultimate load (52 kN), the highest stiffness (12.3 kN/mm), and the highest energy absorption (1748 kNmm).

Fig. 14. Failure pattern of the Slab elements

The geopolymer slab exhibited a lower ductility index than the cement slab due to its denser, more rigid aluminosilicate matrix. In contrast, the SSW-blended slab achieved the highest ductility index (4.20), indicating a greater deformation capacity before failure. However, despite its high ductility index, the SSW slab exhibited the lowest deformability factor and energy absorption capacity, suggesting that deformation became localized after cracking rather than being effectively redistributed throughout the slab. In contrast, the CS-blended slab demonstrated the most balanced post-cracking performance by combining the highest ultimate load (52 kN), highest stiffness (12.3 kN/mm), and highest energy absorption capacity (1748 kNmm). These results indicate that the CS-blended slab possessed superior toughness and post-cracking resistance, enabling it to sustain higher loads while effectively dissipating energy before failure.

The SSW slab merits particular attention because its ductility and deformability indices point in opposite directions: it recorded the highest ductility index yet the lowest deformability factor (0.42) and the lowest energy absorption capacity. These metrics are not contradictory once their definitions are recalled. The ductility index is the ratio of ultimate to first-crack deflection. It is inflated here by the slab's unusually low first-crack load. In contrast, the deformability factor and energy absorption capacity reflect the slab's ability to redistribute stress and dissipate energy across the entire loading history. Read together, these results indicate that deformation in the SSW slab localizes early rather than spreading through the section, so that a large nominal deflection ratio coexists with limited overall toughness. The implication for design is important: a high ductility index alone does not guarantee ductile, energy-absorbing failure, and the deformability factor and energy absorption capacity provide a more reliable measure of post-crack reserve. These mechanistic differences translate into distinct application niches. The CS-blended geopolymer slab offers the most balanced profile, high strength, high stiffness, and the highest energy absorption, making it the preferred choice for load-dominated structural elements. The SSW-blended slab is better regarded as a strength- and deflection-tolerant mix, suited to situations where large recoverable deflection is acceptable but high toughness is not the governing requirement. The plain geopolymer slab delivers the most uniform post-crack response and therefore the best deformability factor. In every case, the bamboo reinforcement performed satisfactorily, sustaining the imposed flexural demand without bond failure, which supports its use as a low-carbon substitute for steel in lightly to moderately loaded slabs.

Higher stiffness generally contributes to reduced service-load deflections and improved structural stability, while adequate ductility and energy absorption enable structural members to sustain inelastic deformation without sudden failure. Among the investigated specimens, the CS-blended geopolymer slab exhibited the most balanced structural response, combining the highest stiffness, ultimate load, and energy absorption capacity. These characteristics indicate enhanced structural robustness and improved resistance to progressive crack propagation under increasing loads. Although the SSW-blended slab exhibited the highest ductility index, its comparatively lower deformability factor and energy absorption capacity suggest that deformation became localized after cracking.

Consequently, the measured ductility and energy absorption characteristics cannot be directly extrapolated to seismic or cyclic loading conditions, where repeated load reversals govern structural performance. The seismic behavior of bamboo-reinforced GPC depends on additional parameters such as hysteretic energy dissipation, cyclic stiffness degradation, bond deterioration between bamboo and concrete, residual displacement, and low-cycle fatigue resistance, which were not investigated in the present study. Therefore, cyclic and pseudo-static testing, together with analytical and reliability-based investigations, are recommended before the proposed slab system can be considered for earthquake-resistant structural applications. Nevertheless, the experimental results presented herein provide valuable baseline data for future seismic assessment and the development of design recommendations for sustainable bamboo-reinforced GPC structures. Beyond these structural metrics, the broader value of the mixes lies in their sustainability. Each geopolymer slab eliminates Portland cement, while the SSW and CS mixes additionally divert industrial by-products from landfill and reduce demand for natural coarse and fine aggregate. Combined with rapidly renewable bamboo reinforcement, the outcome is a composite slab whose strength is maintained or improved even as its reliance on the two most carbon-intensive constituents of conventional reinforced concrete - cement and steel is removed. These findings should nevertheless be interpreted within the scope of the present program: each conclusion rests on a single representative slab per mix tested under short-term monotonic loading. The long-term durability of bamboo reinforcement, including moisture movement, creep, and the integrity of the bamboo–matrix bond, warrants dedicated investigation before field application.

Although the SSW-blended slab exhibited the highest ductility index, it recorded the lowest energy absorption capacity among the investigated specimens. This behavior can be explained from the definitions of the two parameters. The ductility index is calculated as the ratio of the ultimate deflection to the deflection at first cracking and therefore reflects the relative deformation capacity after crack initiation. In contrast, the energy absorption capacity corresponds to the total work done during loading, represented by the area under the load-deflection curve. Consequently, a specimen may exhibit a relatively high ductility index because of large ultimate deflections while simultaneously possessing a lower energy absorption capacity if the sustained load levels after cracking remain comparatively low. Therefore, these two parameters describe different aspects of structural behavior and should not be interpreted as directly proportional. It should be noted that the present interpretation is based on the experimentally measured global structural response under monotonic loading. Since fracture mechanics tests and crack propagation measurements were beyond the scope of this study, the underlying fracture processes could not be directly quantified.

6. Limitation

Although the present study shows the structural feasibility of bamboo-reinforced GPC slabs incorporating SSW and CS, their practical implementation is currently constrained by the absence of comprehensive structural design provisions. Existing reinforced concrete design standards, including IS 456:2000 [70] and ACI 318 [71], were developed for steel-reinforced Portland cement concrete and therefore do not address the mechanical behavior of bamboo reinforcement or alkali-activated concrete. Similarly, IS 17452 [72] guides the production and quality assurance of alkali-activated concrete but does not establish structural design equations for reinforced geopolymer members. Consequently, structural design of GPC currently relies on adapting conventional reinforced concrete provisions following experimental validation. Furthermore, no internationally accepted structural design standard presently exists for bamboo-reinforced concrete members. Important design aspects such as bond characteristics, anchorage requirements, development length, durability under varying environmental conditions, creep, shrinkage, moisture movement, long-term stiffness degradation, partial safety factors, and serviceability limits have not yet been sufficiently standardized. The simultaneous use of GPC, bamboo reinforcement, SSW, and CS introduces additional material interactions that remain outside the scope of current design specifications.

Accordingly, the present investigation was regarded as a proof-of-concept experimental study that establishes the structural behavior of an integrated sustainable slab system. The measured flexural response, first-crack load, ultimate load, stiffness, ductility, deformability, and energy absorption provide valuable experimental data for validating numerical models and supporting future reliability-based calibration of design equations. Before widespread structural implementation, additional research addressing long-term durability, bond performance, environmental exposure, cyclic and fatigue loading, fire performance, and reliability analysis is required to facilitate the development of dedicated structural design recommendations and future code provisions for bamboo-reinforced geopolymer concrete.

Future investigations have to be made by incorporating fracture energy measurements, crack mouth opening displacement (CMOD), digital image correlation (DIC), and microstructural characterization to establish the relationship between crack propagation mechanisms and the observed post-cracking behavior.

7. Conclusions

- The compressive strength of all the concrete mixes attained its target strength > 30 MPa. Moreover, a marginal variation in the strength was seen amongst the mixes; this might be attributed to the variation in the material properties.
- The GPC mix showed the greatest resistance to initial cracking, with a first-crack load of 23 kN, which was 26% above the cement mix. The SSW-based slab recorded the lowest value (16 kN, 30% below the GPC mix), while the CS mix matched the cement mix and remained 26% below the GPC mix.
- The CS mix carried the highest ultimate load, 52 kN, representing 6% above the GPC mix and 15.5% above the cement mix. Whereas the SSW mix essentially matched the GPC mix.
- The CS mix was also the stiffest, exceeding the GPC mix by 12% and the cement mix by 36.7%, with the SSW mix 8.5% above the GPC mix.
- The SSW mix recorded the highest ductility index, 4.20, showing 55% above the GPC mix, while the CS mix improved on the GPC mix by 20%.
- The GPC mix achieved the highest deformability factor, 18% above the cement mix. In contrast, the SSW mix recorded the lowest value (0.42, 56% below the GPC mix), reflecting the early localization of deformation despite its high ductility index.
- The CS mix attained the highest energy absorption capacity, 11.4% above the GPC mix and 1.7% above the cement mix; the GPC mix fell 10% below the cement mix, and the SSW mix 14% below the GPC mix. Overall, the CS-blended geopolymer slab delivered the most balanced structural performance, confirming that combining alkali-activation of industrial by-products and bamboo reinforcement is a viable route to sustainable, structurally efficient slab elements.
- Although the proposed bamboo-reinforced geopolymer slab system exhibited promising structural performance, its practical implementation requires future research on long-term durability, bond behavior, reliability-based calibration, and the development of dedicated structural design provisions before widespread engineering adoption.

Acknowledgement

This work has not been published or submitted for publication elsewhere, and it received no external funding.

References

[1] Lu C, Wang K. Natural resource conservation outpaces climate change: Roles of reforestation, mineral extraction, and natural resources depletion. Resour Policy. 2023;86. https://doi.org/10.1016/j.resourpol.2023.104159
[2] Khankhaje E, Kim T, Jang H, Kim CS, Kim J, Rafieizonooz M. A review of utilization of industrial waste materials as cement replacement in pervious concrete: An alternative approach to sustainable pervious concrete production. Heliyon. 2024;10(4):e26188. https://doi.org/10.1016/j.heliyon.2024.e26188
[3] Gebremariam HG, Taye S, Tarekegn AG. Parent Concrete Strength Effects on the Quality of Recycled Aggregate Concrete: A Review. Heliyon. 2024;10(4):e26212. https://doi.org/10.1016/j.heliyon.2024.e26212
[4] Alqarni AS, Abbas H, Al-Shwikh KM, Al-Salloum YA. Treatment of recycled concrete aggregate to enhance concrete performance. Constr Build Mater. 2021;307(8). https://doi.org/10.1016/j.conbuildmat.2021.124960
[5] Caracol C, Kravchanka L, Bravo M, de Brito J, Agrela F, Rosales J. Recycled aggregate concrete using seawater: Optimizing concrete's sustainability. J Build Eng. 2024;97. https://doi.org/10.1016/j.jobe.2024.110841
[6] Alharthai M, Onyelowe KC, Ali T, Qureshi MZ, Rezzoug A, Deifalla A, et al. Enhancing concrete strength and durability through incorporation of rice husk ash and high recycled aggregate. Case Stud Constr Mater. 2025;22. https://doi.org/10.1016/j.cscm.2024.e04152
[7] Evangelista L, de Brito J. Mechanical behaviour of concrete made with fine recycled concrete aggregates. Cem Concr Compos. 2007;29(5). https://doi.org/10.1016/j.cemconcomp.2006.12.004
[8] Ho NY, Lee YP, Lim WF, Zayed T, Chew KC, Low GL, et al. Efficient Utilization of Recycled Concrete Aggregate in Structural Concrete. J Mater Civ Eng. 2013;25(3). https://doi.org/10.1061/(ASCE)MT.1943-5533.0000587
[9] Mohanta NR, Murmu M. Alternative coarse aggregate for sustainable and eco-friendly concrete - A review. J Build Eng. 2022;59:105079. https://doi.org/10.1016/j.jobe.2022.105079
[10] Murmu M, Mohanta NR, Bapure N. Study on the fresh and hardened properties of concrete with steel slag as partial replacement for natural aggregates. Mater Today Proc. 2023. https://doi.org/10.1016/j.matpr.2023.03.151
[11] Mohanta NR, Murmu M. Review on the Utilization of Steel Slag as Alternative Coarse Aggregate in Concrete: Transforming Waste into Wealth. Iran J Sci Technol Trans Civ Eng. 2026;50:2269-304. https://doi.org/10.1007/s40996-025-01981-5
[12] Mohanta NR, Murmu M. Comparative study on the effect of incorporation of Linz-Donawitz slag as coarse aggregate in concrete reinforced with different fibers. Innov Infrastruct Solut. 2024;9(76). https://doi.org/10.1007/s41062-024-01387-8
[13] Mohanta NR, Samantaray S. Study of Combined Effect of Metakaolin and Steel Fiber on Mechanical Properties of Concrete. Pertanika J Sci Technol. 2019;27(3):1381-96.
[14] Pedro D, de Brito J, Evangelista L. Influence of the use of recycled concrete aggregates from different sources on structural concrete. Constr Build Mater. 2014;71. https://doi.org/10.1016/j.conbuildmat.2014.08.030
[15] Rahal K, Alrushaidan M, Almutairi A. Flexural behavior of recycled aggregates concrete beams reinforced with GFRP bars. J Eng Res. 2024. https://doi.org/10.1016/j.jer.2024.12.008
[16] Stochino F, Alibeigibeni A, Zucca M, Valdes M, Concu G, Simoncelli M, et al. Mechanical behavior of composite slabs with recycled concrete aggregates: A preliminary study. Structures. 2024;70. https://doi.org/10.1016/j.istruc.2024.107838
[17] Malešev M, Radonjanin V, Marinković S. Recycled Concrete as Aggregate for Structural Concrete Production. Sustainability. 2010;2(5). https://doi.org/10.3390/su2051204
[18] Azandariani MG, Vajdian M, Javadi M, Parvari A. Durability and compressive strength of composite polyolefin fiber-reinforced recycled aggregate concrete: An experimental study. Compos Part C Open Access. 2024;15. https://doi.org/10.1016/j.jcomc.2024.100533
[19] Haruehansapong S, Khamput P, Yoddumrong P, Thuadao WKV, Abdulmatin A, Senawang W, et al. Enhancement of recycled aggregate concrete properties through the incorporation of nanosilica and natural fibers. Heliyon. 2024;10(22). https://doi.org/10.1016/j.heliyon.2024.e39924

[20] Ige OE, Von Kallon DV, Desai D. Carbon emissions mitigation methods for cement industry using a systems dynamics model. Clean Technol Environ Policy. 2024;26(3):579-97. https://doi.org/10.1007/s10098-023-02683-0
[21] Terán-Cuadrado G, Tahir F, Nurdiawati A, Almarshoud M, Al-Ghamdi SG. Current and potential materials for the low-carbon cement production: Life cycle assessment perspective. J Build Eng. 2024;96. https://doi.org/10.1016/j.jobe.2024.110528
[22] Collins M, Beverley JD, Bracegirdle TJ, Catto J, McCrystall M, Dittus A, et al. Emerging signals of climate change from the equator to the poles: new insights into a warming world. Front Sci. 2024;2:1-20. https://doi.org/10.3389/fsci.2024.1340323
[23] Hardjito D, Wallah SE, Sumajouw DMJ, Rangan BV. On the development of fly ash-based geopolymer concrete. ACI Mater J. 2004;101(6):467-72. https://doi.org/10.14359/13485
[24] Shehata N, Mohamed OA, Sayed ET, Abdelkareem MA, Olabi AG. Geopolymer concrete as green building materials: Recent applications, sustainable development and circular economy potentials. Sci Total Environ. 2022;836:155577. https://doi.org/10.1016/j.scitotenv.2022.155577
[25] Rangan BV. Geopolymer concrete for environmental protection. Indian Concr J. 2014;88(4):41-59.
[26] Vora PR, Dave UV. Parametric studies on compressive strength of geopolymer concrete. Procedia Eng. 2013;51:210-9. https://doi.org/10.1016/j.proeng.2013.01.030
[27] Rifkah, Saloma, Usman F. Compressive and tensile strength of fly ash based lightweight geopolymer concrete with variation of Na2SiO3 and NaOH using expanded polystyrene. Res Eng Struct Mater. 2025;11(6):2983-97.
[28] Habert G, D'Espinose De Lacaillerie JB, Roussel N. An environmental evaluation of geopolymer based concrete production: Reviewing current research trends. J Clean Prod. 2011;19(11):1229-38. https://doi.org/10.1016/j.jclepro.2011.03.012
[29] Obaid HA, Sarhan IA. The effect of permeability and mechanical properties of low-calcium fly ash based geopolymer concrete. Res Eng Struct Mater. 2026;12(2):981-94.
[30] Sarker PK. Analysis of geopolymer concrete columns. Mater Struct Constr. 2009;42(6):715-24. https://doi.org/10.1617/s11527-008-9415-5
[31] Al-Mayali ZMK. Enhancement of mechanical properties and sulfuric acid resistance in slag-based geopolymer mortars via metakaolin incorporation. Res Eng Struct Mater. 2025;11(4):1749-65. https://doi.org/10.17515/resm2025-884me0508rs
[32] Nurjannah SA, Saloma, Usman FA. Performance of geopolymer concrete flat slab with various transverse reinforcement in resisting punching shear. Res Eng Struct Mater. 2026.
[33] Salas DA, Ramirez AD, Boero HBAJ. Life cycle assessment of geopolymer concrete. Constr Build Mater. 2018;190. https://doi.org/10.1016/j.conbuildmat.2018.09.123
[34] Zhang HY, Kodur V, Wu B, Yan J, Yuan ZS. Effect of temperature on bond characteristics of geopolymer concrete. Constr Build Mater. 2018;163:277-85. https://doi.org/10.1016/j.conbuildmat.2017.12.043
[35] Koymatcik C, Ozkaymak M, Selimli S. Recovery of iron particles from waste water treatment plant of an iron and steel factory. Eng Sci Technol an Int J. 2018;21(3):284-8. https://doi.org/10.1016/j.jestch.2018.04.008
[36] Ajayi SO, Oyedele LO, Akinade OO, Bilal M, Alaka HA, Owolabi HA, et al. Attributes of design for construction waste minimization: A case study of waste-to-energy project. Renew Sustain Energy Rev. 2017;73:1333-41. https://doi.org/10.1016/j.rser.2017.01.084
[37] Gavilan RM, Bernold LE. Source Evaluation of Solid Waste in Building Construction. J Constr Eng Manag. 1994;120(3). https://doi.org/10.1061/(ASCE)0733-9364(1994)120:3(536
[38] Formoso CT, Soibelman L, De Cesare C, Isatto EL. Material Waste in Building Industry: Main Causes and Prevention. J Constr Eng Manag. 2002;128(4). https://doi.org/10.1061/(ASCE)0733-9364(2002)128:4(316
[39] Silva G, Kim S, Aguilar R, Nakamatsu J. Natural fibers as reinforcement additives for geopolymers - A review of potential eco-friendly applications to the construction industry. Sustain Mater Technol. 2020;23:e00132. https://doi.org/10.1016/j.susmat.2019.e00132
[40] Dey A, Chetia N. Experimental study of Bamboo Reinforced Concrete beams having various frictional properties. Mater Today Proc. 2018;5(1). https://doi.org/10.1016/j.matpr.2017.11.103
[41] Qaiser S, Hameed A, Alyousef R, Aslam F, Alabduljabbar H. Flexural strength improvement in bamboo reinforced concrete beams subjected to pure bending. J Build Eng. 2020;31. https://doi.org/10.1016/j.jobe.2020.101289
[42] Ramaani P, Natarajan B, Rajendran RR. An in-depth assessment of the structural integrity and advantages of bamboo-reinforced cement concrete elements (BRCC) with utilizing an alternative binding material: a comprehensive evaluation. Rev Mater. 2024;29(3). https://doi.org/10.1590/1517-7076-rmat-2024-0067

[43] Agarwal A, Nanda B, Maity D. Experimental investigation on chemically treated bamboo reinforced concrete beams and columns. Constr Build Mater. 2014;71. https://doi.org/10.1016/j.conbuildmat.2014.09.011
[44] Prem Kumar V, Vasugi V. Bamboo materials in cement, geopolymer and reinforced concrete as sustainable solutions for better tomorrow. IOP Conf Ser Earth Environ Sci. 2020;573(1). https://doi.org/10.1088/1755-1315/573/1/012036
[45] A SK, A PRMR, Awoyera PO. Strength properties of bamboo and steel reinforced concrete containing manufactured sand and mineral admixtures. J King Saud Univ - Eng Sci. 2017;29(4). https://doi.org/10.1016/j.jksues.2016.12.003
[46] Govindan B, Ramasamy V. Performance assessment on bamboo reinforced concrete beams. Innov Infrastruct Solut. 2022;7. https://doi.org/10.1007/s41062-021-00616-8
[47] Terai M, Minami K. Fracture Behavior and Mechanical Properties of Bamboo Reinforced Concrete Members. Procedia Eng. 2011;10. https://doi.org/10.1016/j.proeng.2011.04.492
[48] Moroz JG, Lissel SL, Hagel MD. Performance of bamboo reinforced concrete masonry shear walls. Constr Build Mater. 2014;61. https://doi.org/10.1016/j.conbuildmat.2014.02.006
[49] Mali PR, Datta D. Experimental evaluation of bamboo reinforced concrete slab panels. Constr Build Mater. 2018;188:1092-100. https://doi.org/10.1016/j.conbuildmat.2018.08.162
[50] Mali PR, Datta D. Experimental evaluation of bamboo reinforced concrete beams. J Build Eng. 2020;28. https://doi.org/10.1016/j.jobe.2019.101071
[51] Anto A, Augustin A, Ratheesh R, Xavier CB. Flexural behavior of the untreated plain bamboo reinforced concrete beam under four-point loading. Mater Today Proc. 2023. https://doi.org/10.1016/j.matpr.2023.03.543
[52] Haryanto Y, Wariyatno NG, Hu HT, Han AL, Hidayat BA. Investigation on structural behaviour of bamboo reinforced concrete slabs under concentrated load. Sains Malaysiana. 2021;50(1):227-38. https://doi.org/10.17576/jsm-2021-5001-22
[53] Adegbemileke SA, Usidamen D, Ogirigbo OR, Nwankwo E. Mechanical properties and flexural behaviour of bamboo-reinforced concrete beams. J Appl Sci Environ Manag. 2025;29(7):2229-39. https://doi.org/10.4314/jasem.v29i7.23
[54] Tariq M, Haydar S, Khushnood RA, Haq EU, Hameed A, Khan N. Advancing sustainable construction: Experimental study of concrete beams reinforced with chemically treated bamboo and enhanced interfacial bonding using nanotechnology. J Build Eng. 2025;9. https://doi.org/10.1016/j.jobe.2024.111552
[55] Asres MA, Zerayohannes G, Zekaria A, Nuramo DA. Bamboo Fiber Impact on the Long-Term Mechanical Properties of Concrete. J Nat Fibers. 2026;23(1). https://doi.org/10.1080/15440478.2025.2609334
[56] Wibowo A, Wijatmiko I, Nainggolan CR. Bamboo reinforced concrete slab with styrofoam lamina filler as solution of lightweight concrete application. MATEC Web Conf. 2017. https://doi.org/10.1051/matecconf/201710105012
[57] Terlumun S, Michael OE, Samuel OA, Okafor FO, Habibu AS. Investigating the flexural performance of bamboo reinforced concrete beams. J Biodivers Environ Res. 2024.
[58] Muhtar M, Dewi SM, Munawir AA. Bond-slip improvement of bamboo reinforcement in concrete beam using hose clamps. In: Proceedings of The 2nd International Multidisciplinary Conference. 2016.
[59] Kanagaraj B, Anand N, Johnson Alengaram U, Samuvel Raj R, Kiran T. Exemplification of sustainable sodium silicate waste sediments as coarse aggregates in the performance evaluation of geopolymer concrete. Constr Build Mater. 2022;330:127135. https://doi.org/10.1016/j.conbuildmat.2022.127135
[60] Kanagaraj B, Anand N, Raj RS, Lubloy E, Ash F, Ash RH. Performance evaluation of sodium silicate waste as a replacement for conventional sand in geopolymer concrete. J Clean Prod. 2022;375:134172. https://doi.org/10.1016/j.jclepro.2022.134172
[61] ASTM International. ASTM C143 / C143M: Standard Test Method for Slump of Hydraulic-Cement Concrete. Annual Book of ASTM Standards. 2020.
[62] Bureau of Indian Standards. IS 516: Method of Tests for Strength of Concrete - Specifications. New Delhi, India; 2021.
[63] Canadian Standards Association. CSA S806-12: Design and construction of building structures with fibre-reinforced polymers. 2012.
[64] Kanagaraj B, Anand N, Raj RS, Lubloy E. Techno-socio-economic aspects of Portland cement, Geopolymer, and Limestone Calcined Clay Cement (LC3) composite systems. Constr Build Mater. 2023;398:132484. https://doi.org/10.1016/j.conbuildmat.2023.132484
[65] Alsalman A, Assi LN, Kareem RS, Carter K, Ziehl P. Energy and CO2 emission assessments of alkali-activated concrete and Ordinary Portland Cement concrete: A comparative analysis of different grades of concrete. Clean Environ Syst. 2021;3:100047. https://doi.org/10.1016/j.cesys.2021.100047

[66] Mohanta NR, Murmu M. Performance assessment of Linz-Donawitz slag as alternative coarse aggregate in concrete: a comprehensive study on mechanical and durability properties. Innov Infrastruct Solut. 2023;8(281). https://doi.org/10.1007/s41062-023-01257-9

[67] Mohanta NR, Murmu M. Evaluating the cumulative influence of Linz-Donawitz slag and glass fibre incorporation in concrete: a durability study. Aust J Civ Eng. 2025;142-73. https://doi.org/10.1080/14488353.2025.2563900

[68] Mohanta NR, Murmu M. Exploring the combined impact of coarse linz-donawitz slag and basalt fiber on the properties of concrete. J Build Pathol Rehabil. 2025;10(20). https://doi.org/10.1007/s41024-024-00528-x

[69] Mohanta NR, Murmu M. Evaluating the Co-relationship between the mechanical properties of steel slag aggregate concrete reinforced with steel fiber. Eng Res Express. 2025;7(2). https://doi.org/10.1088/2631-8695/ade6cb

[70] Bureau of Indian Standards. IS 456: Plain and Reinforced Concrete - Code of Practice. New Delhi, India; 2000. p. 1-114.

[71] American Concrete Institute. ACI 318-19: Building Code Requirements for Structural Concrete and Commentary (ACI 318R-19). Farmington Hills, MI; 2019. 988 p.